J IRAN CHEM SOC (2015) 12:2015–2021
DOI 10.1007/s13738-015-0676-y

ORIGINAL PAPER

The $Ag_{core}Pd_{shell}$ bimetallic nanoparticles: simple biological synthesis and characterization

Khalil Farhadi[1] · Reza Emamali Sabzi[1] · Mehrdad Forough[1] · Atefeh Pourhossein[1] · Rahim Molaei[1] · Rokhsareh Ebrahimi[1]

Received: 11 September 2014 / Accepted: 2 June 2015 / Published online: 18 June 2015

Abstract In this work and for the first time, bimetallic Ag–Pd nanoparticles equipped with a core–shell structure were prepared biologically by employing a galvanic displacement reaction in which the added $PdCl_2$ reacts with an Ag nanotemplate containing an adsorbed soaproot (*Acanthe phylum bracteatum*) extract. Four samples with different Ag/Pd molar ratios of 100:2, 100:5, 100:10 and 100:15 were prepared to synthesize the bimetallic nanoparticles with a core–shell structure. The bimetallic Ag–Pd nanoparticles were characterized using UV–visible spectroscopy (UV–Vis), X-ray diffraction (XRD), scanning electron microscopy with an energy-dispersive X-ray spectroscopy (SEM–EDX), transmission electron microscopy (TEM) and Fourier transform infrared spectroscopy (FTIR) analysis. The results from UV–Vis revealed an optimal molar ratio of 100:15 for Ag/Pd, which is appropriate to prepare bimetallic Ag–Pd nanoparticles with the core–shell structure. The results of FTIR and XRD confirmed the pure bimetallic Ag–Pd nanoparticles formation. The images prepared by TEM depicted spherical and uniformly shaped nanoparticles without any agglomeration and a particle size of 15 nm.

Keywords Biosynthesis · Bimetallic · Ag–Pd nanoparticles · Soaproot · Core–shell

✉ Khalil Farhadi
khalil.farhadi@yahoo.com; kh.farhadi@urmia.ac.ir

[1] Department of Analytical Chemistry, Faculty of Chemistry, Urmia University, Urmia, Iran

Introduction

Recently, the development of simple methods to prepare nano-sized particles has drawn significant attention because of their promising applications in unusual size-dependent properties. The synthesis of nanoparticles has been followed intensively not only because of their fundamental scientific benefits, but also for many technological applications [1]. So far, the biosynthesis of nanoparticles has received considerable attention due to a growing need to develop environment-friendly techniques in material synthesis. The green synthesis provides advantages for physical and chemical methods, as it is environmentally friendly, cost-effective and easily scaled up for large-scale synthesis where there is no need to use high pressure, energy, temperature treatment and hazardous chemicals [2–4]. Metal nanoparticles show unusual behavior compared to bulk metals, because of their extremely small size and large specific surface area [5–7]. In particular, the bimetallic nanoparticles which are regarded as an interesting area of research are found to have excellent activities compared to those of pure metal nanoparticles on catalysis applications, surface plasma band energies and magnetic materials [8–13]. From the technological and scientific points of view, the bimetallic nanoparticles are composed of two different metal elements which are more appropriate and efficient than the monometallic nanoparticles where the synergistic effect is expected [14–16]. Considering the diverse structural aspects, it is important to control the homogeneity, dispersion and alloying extent, as they each have a profound influence on surface properties affecting stability and catalytic activity of the bimetallic nanoparticles [17–19]. There are two main types of bimetallic nanoparticles called core–shell and alloyed nanoparticles. The core–shell bimetallic nanoparticles have

unique catalytic, optical and electronic properties different from those of corresponding monometallic particles and alloyed nanoparticles [20–22]. Also, they have important biological applications in DNA sequencing, SERS, etc., [19, 23]. Several methods have been developed for fabrication of the bimetallic nanoparticles. For example, successive reduction [24] and reduction of co-complexes [25] co-reduce metal ion precursors with alcohol [26], citrate [27], borohydride [28], hydrazine [29], etc. Other synthesis methods such as sono-chemical [29, 30], hydrothermal [31] and laser ablation [32] methods are also considered. Although a lot of work has been done on the fabrication of noble metal alloys, there are only a few reports on the bimetallic nanoparticles of palladium with silver [33–39]. On the other hand, the synthesis and fabrication of bimetallic nanoparticles would benefit from the development of clean, nontoxic and environmentally acceptable ''green chemistry'' procedures, probably involving organisms ranging from bacteria to fungi and plants. In this study, we explored for the first time the potential of a non-pathogenic biological system for the biosynthesis of Ag–Pd bimetallic nanomaterials. To the best of our knowledge, there are no other reports on the reduction of aqueous metal ions from *Astraglmanna* or any other manna for preparation of bimetallic nanoparticles.

Ag/Pd bimetallic nanoparticles (random alloy or core–shell structures) have been the center of attention in this case. These systems were found to act as selective hydrogenation catalysts [40, 41] and also showed successful application as a novel activator for electron-free copper and Ni deposition [42, 43]. In addition, the Ag/Pd bimetallic nanoparticles alloy is employed industrially as an H_2 purification membrane [44].

Being motivated by these aspects, we became interested in studying the Ag/Pd bimetallic nanoparticles and succeeded in introducing a novel and simple method for biological synthesis of $Ag_{core}Pd_{shell}$ bimetallic nano-sized particles for the first time. In the current study, first, Ag–Pd core–shell nanostructures were successfully deposited in an environmentally friendly way to stabilize and reduce them via a green route by applying the reduction method of silver (I) ions with an aqueous extract derived from *Astraglmanna* as a non-toxic and eco-friendly material. Next, an aqueous extract of soaproot (*Acanthe phylum bracteatum*) was used as a stabilizer agent. Finally, palladium (II) ions were added to perform the galvanic replacement reaction. This motivated us to deposit the possible bio-reduced ions of silver into the nanoparticles.

The word "manna" has generally been used to describe saccharine exudations from a number of different plants belonging to various families. *Astraglmanna* (*Gaz-angabin* or *Astragalus adscendens*) is a sweet liquid with pharmaceutical benefits that is depleted by Psylloidea insects after they nourish on the *Quercus castaneifolia* plant extract. It is free of nitrogen, sulfur, tannin, alkaloids and halogens [45, 46].

The structure and morphology of synthesized bimetallic nanoparticles were characterized by UV–visible spectroscopy (UV–Vis), X-ray diffraction (XRD), transmission electron microscopy (TEM) and scanning electron microscopy with an energy-dispersive X-ray spectroscopy (SEM–EDX) and Fourier transform infrared spectroscopy (FTIR) analysis.

Materials and methods

Materials and reagents

Silver nitrate ($AgNO_3$ 99.8 %) was purchased from Merck (Darmstadt, Germany). Palladium (II) chloride ($PdCl_2$) as the source of palladium ions was received from Fluka. Concentrated HCl was purchased from Merck (Darmstadt, Germany). Distilled de-ionized water (DW) was used throughout the reactions. The *Astraglmanna* and soaproot (*Acanthe phylum bracteatum*) were used to make extracts.

Preparation of biomass

First, the soaproot extract was prepared by taking 5 g of thoroughly washed plant material to a 250-mL Erlenmeyer flask with 100 mL of de-ionized water. Next, the mixture was boiled for 20 min in an oil bath at 80 °C. After that, the mixture was filtered and centrifuged at 8000 rpm for 60 min. Then, *Astraglmanna* was collected and powdered to obtain the extract of manna. Later, about 5 g of manna was transferred into a 150-mL beaker containing 100-mL DW. The mixture was then boiled for 15 min in an oil bath at 80 °C. Finally, the mixture was stirred for 30 min at the same temperature and then filtered and centrifuged.

Synthesis of Ag–Pd bimetallic nanoparticles

To prepare $Ag_{core}Pds_{hell}$ bimetallic nanoparticles, first, 20 mL of freshly prepared extract of *Astraglmanna* was added to 100 mL of 1 mM aqueous solution of silver nitrate and kept in a water bath at 75 °C for 15 min. Next, 20 mL of the prepared extract of soaproot was added to the mixture and incubated in a rotary shaker for 2 h under dark conditions. After that, an appropriate amount of 1 mM aqueous solution of palladium chloride (2, 5, 10, 15 mL) was gradually added to a stirred solution of Ag nanoparticles at room temperature (the samples prepared from the aqueous solution of $AgNO_3/PdCl_2$ mixture are in molar ratios of 100:2, 100:5, 100:10 and 100:15, respectively). Then, the resulting bimetallic nanoparticles

were filtered and washed three times with DW. Finally, the powder was dried at 150 °C for 2 h in an oven. Also, for comparison, the Pd nanoparticles were produced through a method similar to the synthesis of Ag nanoparticles [47].

Particle characterization

The size, morphology and dispersion of the $Ag_{core}Pd_{shell}$ bimetallic nanoparticles were manifested and analyzed by transmission electron microscopy (TEM). These images were taken by a Philips EM 208 electron microscope at 100 keV. The samples for TEM were prepared by placing known drops of aqueous suspension after being ultrasounded on carbon-coated copper grids and allowing water to be evaporated completely prior to measurement. The UV–Vis absorbance spectra of the monometallic and bimetallic nanoparticles suspensions were recorded on a double beam, T80+ UV–Vis spectrophotometer PG (China) with 1-cm quartz cells by using wavelength between 300 and 800 nm at a resolution of 5 nm. A scanning electron micrograph (SEM) was recorded for the further characterization and morphology of the bimetallic nanoparticles using a Philips XL-30 electron microscope operating at 30 kV and equipped with an energy-dispersive X-ray spectrometer (EDX). The X-ray diffraction (XRD) of the bimetallic nanoparticles was determined using X-ray diffractometer (XRD; Philips PW-180, Germany) operating at a voltage of 40 kV with Cu Kα (1.5418 Å) radiation. Freeze drying of the samples for SEM and XRD tests was carried out using an ALPHA 1-4 freeze dryer (CHRIST, Germany) under vacuum conditions at −50 °C for 40 h. The Fourier transform infrared spectroscopy (FTIR) analysis was investigated using Thermo Nicolet-Nexus® 670 FTIR instrument (USA) in the transmittance mode between 400 and 4000 cm^{-1}.

Results and discussion

For the synthesized bimetallic nano-sized particles, the UV–Vis spectrum is a useful and simple tool to define the nanostructure as a core–shell or mixed alloys structure. In general, if the outer layer is pure metal and substantial, the characteristic SPR band presenting the outer metal will be considered more [48].

Figure 1 shows the UV–Vis spectra of the metallic nanoparticles with different initial molar ratios of Ag/Pd. Theoretically and according to Mie theory [48], a surface plasmon resonance (SPR) band of monometallic Ag nanoparticles at 435 nm and the absence of SPR band of monometallic Pd NPs from 300 to 800 nm are consistent with previous reports [47]. In Fig. 1, a distinct band is observed

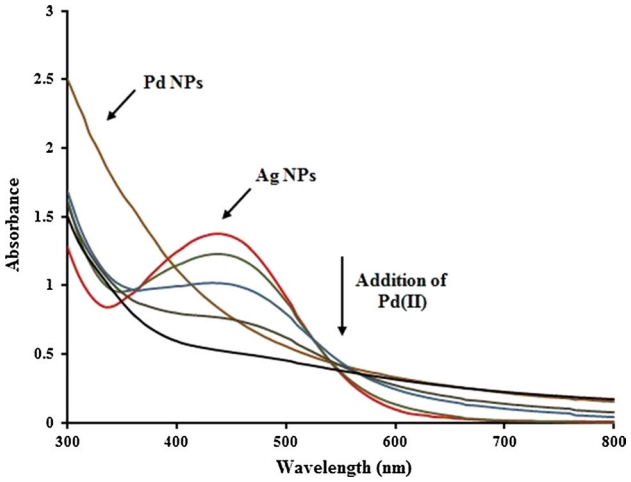

Fig. 1 UV–visible spectra of biosynthesized Ag nanoparticles, Pd nanoparticles and bimetallic nanoparticles with different initial molar ratios of Ag/Pd (100:2, 100:5, 100:10, 100:15)

at 435 nm for Ag colloid that must be due to localized surface plasmon resonance (LSPR) excitation of Ag nanoparticles. It is notable that this band is gradually weakened without any shift or distortion as Pd is added to form Ag/Pd (100:2), Ag/Pd (100:5), Ag/Pd (100:10) and Ag/Pd (100:15) nanoparticles. The UV–Vis absorption is not seen at all of the pure Pd colloids.

Through increasing concentration of palladium ions in bimetallic nanoparticles, the silver peak at 435 nm is reduced and, eventually, no distinct absorption peaks are observed in the optimal molar ratio of Ag/Pd (100:15). It is plausible that Pd atoms dominate and enrich the prepared Ag/Pd nanoparticles surface. UV–Vis spectra of metallic nanoparticles indicate the formation of $Ag_{core}Pd_{shell}$ bimetallic nanoparticles. The same results have been reported by other researchers as well [49, 50]. Therefore, according to the UV–Vis results, it seems that to obtain the core–shell structure of the Ag/Pd nanoparticles by this method, the optimal molar ratio of Ag/Pd is 100:15.

The crystalline structure and phases of the samples were determined by X-ray diffraction (XRD) analysis. The XRD patterns of the biosynthesized Ag–Pd bimetallic nanoparticles with molar ratio of 100:15 are shown in Fig. 2b and for comparison. The XRD pattern of the monometallic Pd and the Ag nanoparticles is also displayed in Fig. 2a, c, respectively. In Fig. 2c, the peaks of the Ag monometals appeared at 2θ values of 37.7839°, 44.0117° and 64.3421°, corresponding to diffraction planes (111), (200) and (220) from standard Inorganic Crystal Structure Database (ICSD) card (01-087-0597). In Fig. 2a, the characteristic peaks of the produced powder appeared at 2θ values of 38.5588° and 65.1190°, corresponding to diffraction planes of the Pd phase (111) and (220) from

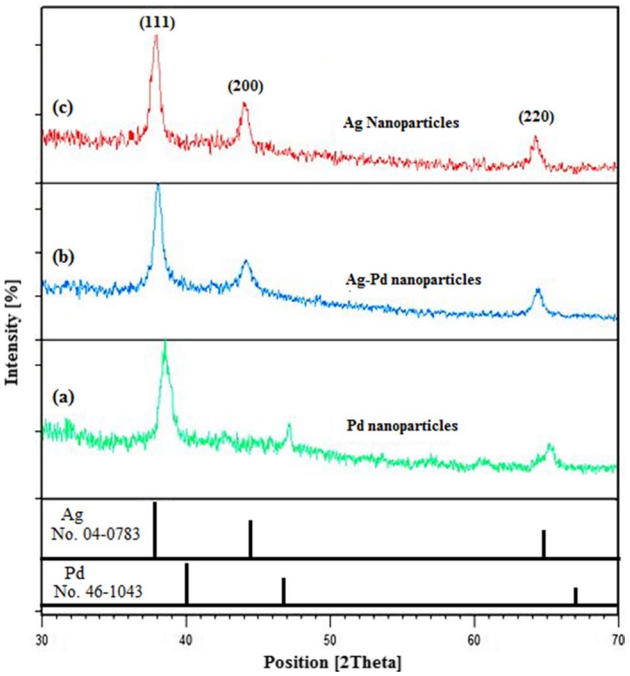

Fig. 2 X-ray diffraction pattern (XRD) of the biosynthesized palladium nanoparticles (**a**), Ag–Pd bimetallic nanoparticles (**b**) and Ag nanotemplates (**c**). Bulk Ag and Pd from the Joint Committee Powder Diffraction Standard (JCPDS) were also included for comparison

standard ICSD card (01-087-0637), and 2θ: 47.1494° corresponding to diffraction planes of Pd nanoparticles (200) that belong to the standard ICSD card (01-087-0645). It is clear that the diffraction line of Ag–Pd bimetallic nanoparticles appeared at 2θ values between the Ag and Pd nanoparticle lines. So, in Fig. 2b, with addition of palladium ions to Ag nanotemplates, all the angles relating to planes (111), (200) and (220) were diverted toward the larger angles of 38.0627°, 44.1239° and 64.3608° compared to the Ag nanotemplates indicating the formation of Ag/Pd bimetallic structure. As seen in Table 1, the lattice constant of the Ag–Pd bimetallic nanoparticles increased compared to that of Pd nanoparticles, which is between Ag and Pd nanoparticles resulting from surface stress. Similar results were also observed by other authors [39, 50]. Furthermore, as shown in Fig. 2b, the peak intensities almost increased in all the angles by addition of palladium to silver (Ag/Pd 100:15).

This increase in peak intensity shows that the crystallization of Ag/Pd nanoparticles has increased as well. Pd and Ag monometallic nanoparticles and Ag–Pd bimetallic nanoparticles have a face-centered cubic (fcc) structure and a space group: Fm3 m. Regarding the XRD data (Fig. 2), the crystallite size (D) of the prepared particles was calculated using the Debye–Scherrer equation:

$$D = \frac{K\lambda}{\beta \mathrm{COS}\theta}, \tag{1}$$

where β is the breadth of the observed diffraction line at its half-intensity maximum (FWHM), K is the so-called shape factor, which usually takes a value of about 0.9, and λ is the wavelength (1.5418 Å) of the X-ray source used in XRD [51]. The average crystallite size of nanoparticles was calculated in diffraction planes (111), (200) and (220). As seen in Table 1, the average crystallite size of Ag–Pd bimetallic nanoparticles with molar ratio of Ag/Pd 100:15 is lower than the Ag and Pd nanoparticles and is about 11.43, 14.4 and 14.37 nm, respectively. Also, the Joint Committee Powder Diffraction Standard (JCPDS) data of silver (No. 04-0783) and palladium (No. 46-1043) have also been given for comparison. The diffraction peaks of Ag and Pd nanoparticles accorded well with the JCPDS data.

The surface morphology and the chemical composition of the $Ag_{core}Pd_{shell}$ bimetallic nanoparticles in molar ratios of 100:15 were investigated by scanning electron microcopy (SEM) at different magnifications with an energy-dispersive X-ray spectroscopy (EDX) (Fig. 3). As seen in Fig. 3a, b, the particles are spherical, very uniform in shape and dispersed. The chemical composition of the obtained Ag–Pd nanoparticles was determined by energy-dispersive X-ray analysis (EDX) as shown in Fig. 3c. The obtained strong signal in the silver and palladium region confirms the formation of bimetallic nano-sized particles.

The TEM images of the Ag nanoparticles and the $Ag_{core}Pd_{shell}$ bimetallic nanoparticles prepared in the molar ratios of 100:15 are shown in Fig. 4a, b, respectively. As shown in Fig. 4a, b, the particles of Ag and bimetallic Ag/Pd nanoparticles prepared by the same method are spherical, which correspond to SEM. From the TEM images, the green synthesized Ag nanoparticles and the $Ag_{core}Pd_{shell}$ bimetallic nanoparticles include nanometric particles which are very small in size with a diameter of about 9–60 and

Table 1 Results of the XRD analysis

Sample	2θ of planes at			Lattice constant (Å)/(111)	Crystallite size (nm)			Average crystallite size (nm)
	(111)	(200)	(220)		(111)	(200)	(220)	
Ag	37.7839°	44.0117°	64.3421°	4.1240	13.8	13.4	16	14.4
Pd	38.5588°	47.1494°	65.1190°	4.0516	11.2	22	9.9	14.37
Ag/Pd (100:15)	38.0627°	44.1239°	64.3608°	4.0950	14.1	10.2	10	11.43

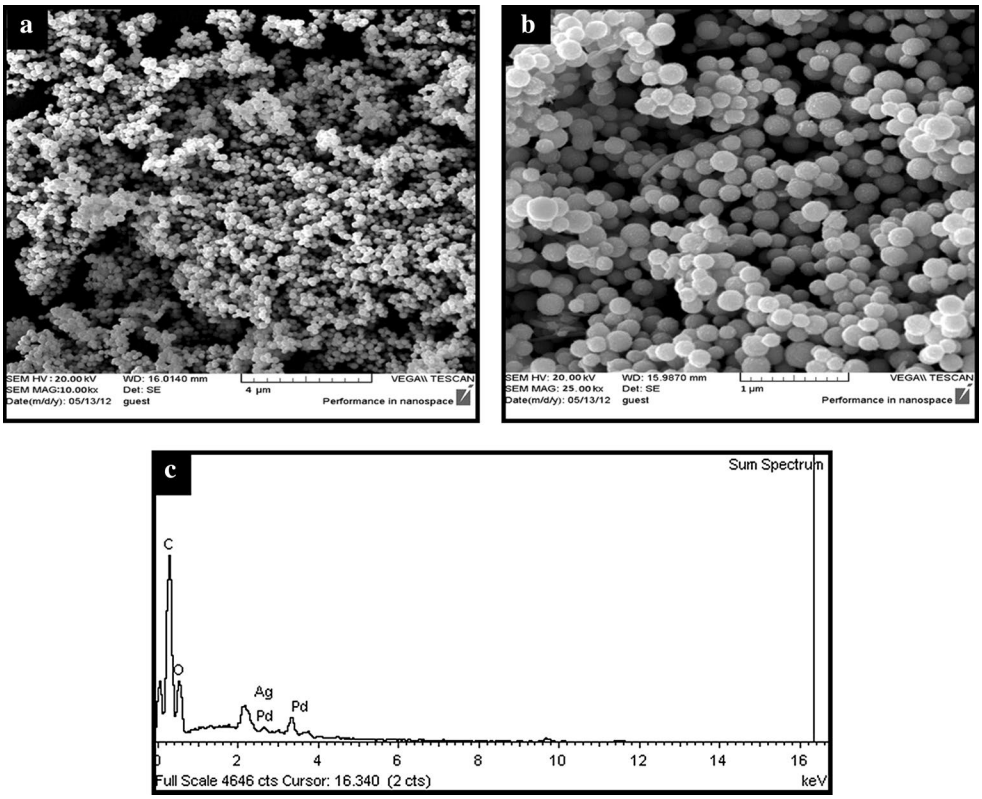

Fig. 3 SEM images (**a**, **b**) and EDX (**c**) analysis of the prepared Ag–Pd bimetallic NPs

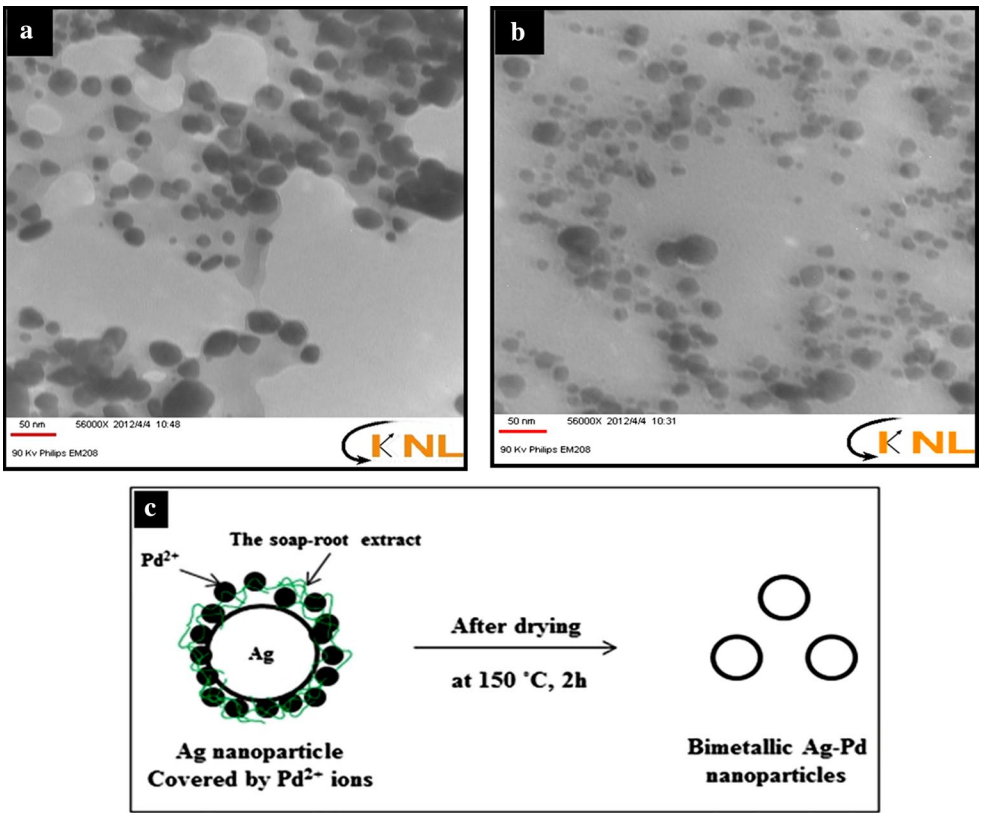

Fig. 4 TEM images (**a**, **b**) and schematic of controlled particle size reduction of Ag–Pd bimetallic nanoparticles in the galvanic replacement reaction between $PdCl_2$ and Ag nanoparticles in the presence of soaproot extract (**c**)

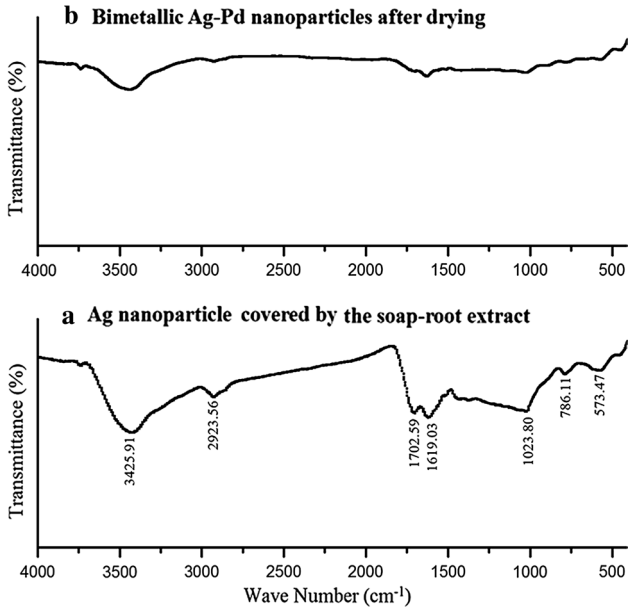

Fig. 5 FT-IR spectra of Ag nanoparticles covered by the soaproot extract (**a**) and Ag–Pd bimetallic nanoparticles after drying (**b**)

5–35 nm, respectively. In the galvanic replacement reaction, it has been previously reported by the authors [52, 53] that addition of metal ions to metal nanoparticles dissolves a part of metallic nanotemplate and changes the initial morphology and size of the nanotemplate. A typical example for this case is the addition of $HAuCl_4$ to Ag nanocubes [54].

Wang et al. [54] showed that when $HAuCl_4$ is added, a small pit is formed on the surface of the Ag nanocubes and changes their morphology. Also, they observed that the size of the nanoparticles increases to about 10–20 % over the initial cubic size. On the contrary, in our green synthesis, we found that the size of the Ag nanotemplate reduces when $PdCl_2$ is added to it, but the morphology of the Ag nanoparticles does not change after adding $PdCl_2$ and retains its spherical shape. This decrease in size of the Ag nanoparticles in the $Ag_{core}Pd_{shell}$ bimetallic nanoparticles was controlled well by the soaproot extract. Also, the unchanged morphology of the Ag nanotemplate after adding Pd^{2+} ions could be attributed to the presence of the extract on the nanotemplate. Figure 4c shows the schematic controlled particle size reduction of the Ag–Pd bimetallic nanoparticles in the galvanic replacement reaction between $PdCl_2$ and the Ag nanoparticles in the presence of the biomass extract. It can be seen that the soaproot extract, which is placed over the Ag nanoparticles, creates a spatial barrier and controls the dissolution of the Ag nanoparticles. As a result, the galvanic replacement reaction between $PdCl_2$ and the Ag nanoparticles in the presence of the extract causes the formation of hollow Ag nanoparticles to be inhibited. We anticipate that the two layers of silver are consumed for one layer of palladium ions and eventually the bimetallic Ag/Pd nanoparticles are created smaller than the single-metal Ag nanoparticles. The mean diameter of the nanoparticles was calculated by averaging roughly 20 particles. The results indicate that the mean diameter of the Ag nanoparticles and the $Ag_{core}Pd_{shell}$ bimetallic nanoparticles are about 30 and 15 nm, respectively.

To confirm the information from the pure bimetallic nanoparticles and distinguish the different groups based on biomass, FTIR spectra were applied (Fig. 5). Figure 5a shows the FTIR spectra of the Ag nanoparticles covered by the soaproot extract before adding $PdCl_2$. Figure 5b is related to the FTIR spectra of the bimetallic Ag–Pd nanoparticles after drying at 150 °C. Before adding $PdCl_2$, the FTIR spectrum (Fig. 5a) contained a broad band at 3425.91 cm^{-1} due to H_2O stretching vibration, indicating the existence of water absorbed in the sample. The bands centered at 2923.59 and 1023.80 cm^{-1} are related to vibration of C–H and O–C bands, representing the stretching vibration of carboxyl and alkyl groups of Ag-covered and soaproot extract, respectively. Also, the peak located at about 1702.59 cm^{-1} is related to the stretching vibration of carboxyl group (COO^-) and 1612 cm^{-1} to C=O rocking vibrations of the organic amide. In Fig. 5b, the disappearance of the bands after adding and drying $PdCl_2$ indicates the complete removal of the soaproot extract by heating at 150 °C and confirms the formation of the highly pure bimetallic Ag–Pd nanoparticles, which is in good agreement with XRD.

Conclusions

The development of simple methods to prepare nano-sized particles has drawn significant attention because of their promising applications in unusual size-dependent properties. In this study, we reported a novel, green and cost-effective synthesis approach of the bimetallic Ag–Pd nanoparticles with a core–shell structure with small particle size. The $Ag_{core}Pd_{shell}$ bimetallic nanoparticles were fabricated by a galvanic displacement reaction. Several samples with different Ag/Pd molar ratios (100:2, 100:5, 100:10 and 100:15) were prepared. The sample with Ag/Pd in molar ratio of 100:15 was chosen as optimal molar ratio and characterized by a variety of standard analytical techniques. The UV–Vis results showed that through increasing concentration of palladium ions in bimetallic nanoparticles, the LSPR of silver nanoparticles is reduced and finally disappeared in the optimal conditions. The FTIR results showed that the obtained bimetallic $Ag_{core}Pd_{shell}$ nanoparticles were pure, and the XRD patterns confirmed that preparation of nanocrystallized bimetallic particles with fcc structure have

an average crystallite size of about 11.43 nm. The SEM micrographs showed that the bimetallic nanoparticles are spherical and uniform in shape with no agglomeration. In addition, TEM studies revealed that after adding $PdCl_2$ to Ag nanotemplate covered by the soaproot extract, the average size of particles reduced from 30 to 15 nm with no change in morphology of the particles.

This work offers a simple and eco-friendly method for green synthesis of the monometallic and bimetallic nanoparticles with very small particle and crystal size. Following this method, their shape and morphology are under control for different applications.

Acknowledgments We acknowledge the scientific support extended by Kefa Nano Laboratory, Tehran, Iran, for analyzing the samples by TEM and DLS.

References

1. M.P. Pileni, J. Phys. Chem. C **111**, 9019 (2007)
2. D. Bhattacharya, R.K. Gupta, Crit. Rev. Biotechnol. **25**, 199 (2005)
3. S. Li, Y. Shen, A. Xie, X. Yu, L. Qiu, L. Zhang, Q. Zhang, Green Chem. **9**, 852 (2007)
4. J.Y. Song, B.S. Kim, Korean J. Chem. Eng. **25**, 808 (2008)
5. K.J. Klabunde, *Nanoscale materials in chemistry* (Wiley, New York, 2001)
6. G.T. Wei, Z. Yang, C.Y. Lee, H.Y. Yang, C.R. Chris, Wang. J. Am. Chem. Soc. **126**, 5036 (2004)
7. S. Nath, S.K. Ghosh, S. Praharaj, S. Panigrahi, S. Basu, T. Pal, New J. Chem. **29**, 1527 (2005)
8. C. Jo, J. Lee, Y. Jang, Chem. Mater. **17**, 2667 (2005)
9. P.P. Singh, J. Magn. Magn. Mater. **261**, 347 (2003)
10. A. Fortunelli, A.M. Velaso, J. Mol. Struct. (Theochem.) **586**, 17 (2002)
11. S. Spriano, F. Rosalbino, M. Baricco, P.V. Morra, E. Angelini, C. Antonione, J.M. Siffre, P. Marcus, Intermetallics **8**, 299 (2000)
12. X. Zhang, K.Y. Chan, Chem. Mater. **15**, 451 (2003)
13. S.W. Han, Y. Kim, K. Kim, J. Colloid Interface Sci. **208**, 272 (1998)
14. G. Ennas, A. Falqui, S. Marras, C. Sangregorio, G. Marongiu, Chem. Mater. **16**, 5659 (2004)
15. F. Tao, M.E. Grass, Y. Zhang, D.R. Butcher, F. Aksoy, S. Aloni, V. Altoe, S. Alayoglu, J.R. Renzas, C.K. Tsung, Z. Zhu, Z. Liu, M. Salmeron, G.A. Somorjai, J. Am. Chem. Soc. **132**, 8697 (2010)
16. A. Kongkanand, K. Tvrdy, K. Takechi, M.K. Kuno, P.V. Kamat, J. Am. Chem. Soc. **130**, 4007 (2008)
17. I. Srnova-Sloufova, F. Lednicky, A. Gemperle, J. Gemperlova, Langmuir **16**, 9928 (2000)
18. S. Devarajan, B. Vimalan, S. Sampath, J. Colloid Interface Sci. **278**, 126 (2004)
19. M.P. Mallin, C.J. Murphy, Nano Lett. **2**, 1235 (2002)
20. F. Zaera, J. Phys. Chem. B **106**, 4043 (2002)
21. L.R. Hirsch, R.J. Stafford, J.A. Bankson, S.R. Sershen, B. Rivera, R.E. Price, J.D. Hazle, N.J. Halas, J.L. West, Proc. Natl. Acad. Sci. **100**, 13549 (2003)
22. O. Amiri, M. Salavati-Niasaria, S.M. Hosseinpour-Mashkanic, A. Rafieid, S. Bagherie, Mater. Sci. Semicond. Process. **27**, 261 (2014)
23. Y.W. Cao, R. Jin, C.A. Mirkin, J. Am. Chem. Soc. **123**, 7961 (2001)
24. Y. Wang, N. Toshima, J. Phys. Chem. B **101**, 5301 (1997)
25. K. Torigoe, Y. Nakajima, K. Esumi, J. Phys. Chem. **97**, 8304 (1993)
26. N. Toshima, Y. Wang, Langmuir **10**, 4574 (1994)
27. S. Link, Z.L. Wang, M.A. El-Sayed, J. Phys. Chem. B **103**, 3529 (1999)
28. O.M. Wilson, R.W.J. Scott, J.C. Garcia-Martinez, R.M. Crooks, J. Am. Chem. Soc. **127**, 1015 (2005)
29. A. Pal, S. Shah, S. Devi, Colloids Surf. A **302**, 51 (2007)
30. M. Salavati-Niasari, J. Javidi, J. Clust. Sci. **23**, 1019 (2012)
31. A. Sobhani, M. Salavati-Niasari, J. Alloys. Compd. **625**, 26 (2015)
32. Y. Mizukoshi, K. Okitsu, Y. Maeda, T.A. Yamamoto, R. Oshima, Y. Nagata, J. Phys. Chem. B **101**, 7033 (1997)
33. J.H. Hodak, A. Henglein, M. Giersig, G.V. Hartland, J. Phys. Chem. B **104**, 11708 (2000)
34. Y.K. Xiao, B. Weng, G. Yu, J. Wang, B. Hu, Z. Chen, J. Appl. Electrochem. **36**, 807 (2006)
35. C.L. Lee, C.M. Tseng, R.B. Wu, K.L. Yang, Nanotechnology **19**, 215709 (2008)
36. W. Wang, B. Zhao, P. Li, X. Tan, J. Nanopart. Res. **10**, 543 (2008)
37. D. Wang, T. Li, Y. Liu, J. Huang, T. You, Cryst. Growth Des. **9**, 4351 (2009)
38. C.L. Lee, C.M. Tseng, R.B. Wu, S.C. Syu, J. Electrochem. Soc. **156**, 348 (2009)
39. L. Chen, Y. Liu, J. Colloid Interface Sci. **364**, 100 (2011)
40. H. Zea, K. Lester, A.K. Datye, E. Rightor, R. Gulotty, W. Waterman, M, Smith. Appl. Catal. A: Gen. **282**, 237 (2005)
41. P.A. Sheth, M, Neurock, C. M. Smith. J. Phys. Chem. B **109**, 12449 (2005)
42. C.C. Yang, Y.Y. Wang, C.C. Wan, J. Electrochem. Soc. **152**, 96 (2005)
43. C.L. Lee, Y.C. Huang, L.C. Kuo, Electrochem. Commun. **8**, 1021 (2006)
44. D. Wang, T.B. Flanagan, K. Shanahan, J. Phys. Chem. B **112**, 1135 (2008)
45. M. Forough, K. Farhadi, Turkish. J. Eng. Env. Sci. **34**, 281 (2010)
46. D. Burckhardt, P. Lauterer, *The Jumping Plant-Lice of Iran (Homoptera, Psylloidea) (Revue Suisse de Zoologie 100* (Chardin, III, 1993)
47. K. Farhadi, A. Pourhossein, M. Forough, R. Molaei, A. Abdi, A. Siami, J. Chin. Chem. Soc. **60**, 1144 (2013)
48. P. Mulvaney, Langmuir **12**, 788 (1996)
49. L. D'Souza, P. Bera, S. Sampath, J. Colloid Interface Sci. **246**, 92 (2002)
50. C. Yang, C.C. Wan, Y.Y. Wang, J. Colloid Interface Sci. **279**, 433 (2004)
51. R. Jenkins, R.L. Snyder, *Chemical analysis: introduction to X-ray powder diffractometry* (Wiley, New York, 1996)
52. C.L. Lee, C.M. Tseng, R.B. Wu, C.C. Wu, S.C. Syu, Electrochim. Acta **54**, 5544 (2009)
53. C.M. Cobley, Y. Xia, Mater. Sci. Eng., R **70**, 44 (2010)
54. Z. Wang, T.S. Ahmad, M.A. El-Sayed, Surf. Sci. **380**, 302 (1997)